MINERALOGY OF THE IBITIRA EUCRITE AND COMPARISON WITH OTHER EUCRITES AND LUNAR SAMPLES

T. M. STEELE and J. V. SMITH
Department of the Geophysical Sciences
The University of Chicago
Chicago, Illinois 60637

Received

Ibitira meteorite is interpreted as a strongly metamorphosed, unbrecciated, vesicular eucrite with a primary variolitic and secondary hornfelsic texture dominated by 60% pyroxene (bulk composition $En_{37}Fs_{48}Wo_{15}$ exsolved into lamellae several micrometers wide of augite $En_{32}Fs_{27}Wo_{41}$ and pigeonite $En_{40}Fs_{56}Wo_4$) and 30% plagioclase An_{94} (mosaic extinction and variable structural state). Minor phases are 5% tridymite plates one-quarter occupied by plagioclase (An_{94}) inclusions; several % intergrowths of ilmenite and Ti-chromite with trace kamacite $Fe_{99}Co_{0.5}Ni_{0.2}$ and narrow olivine (Fa_{83}) rims; one grain of low-Ti-chromite enclosed in tridymite; trace troilite with kamacite $Fe_{98}Co_{1.0}Ni_{0.9}$. Euhedral ilmenite, Ti-chromite, plagioclase and merrillite in vesicles indicate vapor deposition. These properties can be explained by a series of processes including at least the following: (a) igneous crystallization under pressure low enough to allow vesiculation, (b) prolonged metamorphism, perhaps associated with vapor deposition and reduction, to produce the coarse exsolution of the pyroxene and the coarse ilmenite-chromite intergrowths, (c) strong shock which perhaps melted the plagioclase and tridymite but not the pyroxene, and (d) sufficient annealing to allow crystallization of the plagioclase and tridymite, and partial conversion to the low structural state of the former.

1. Introduction

Because the Ibitira eucrite, unlike other eucrites and howardites, is unbrecciated and has an apparently vesicular texture [1], it promises to provide particularly valuable clues for the parent body or bodies of these achondrites. Because of the similarity between these achondrites and samples from the lunar surface, as noted frequently (e.g. [2], [3]), experience from the latter can be applied to the former. Wilkening and Anders [1] briefly described the mineralogy and track history of Ibitira, and concluded that it originated from a basalt flow 2.5-20 meters thick. Using single crystal X-ray and energy-dispersive electron-probe techniques, we continued their study.

2. General Description and Texture

Two types of samples were available: a) a polished thin-section (area $\approx 1 cm^2$) previously used by Wilkening and Anders [1] and b) small fragments ($\leq$ 2mm) and single mineral grains.

Fig. 1 Fig. 1a shows some general features in the thin section. Equant (0.1-0.2mm) grains of pale-brown pyroxene showing ~ 3-5μm

Fig. 2 exsolution lamellae (Fig. 2a) comprise ~ 60% of the area and are set in an irregular matrix of plagioclase (30%). Sub-rounded holes up to 1mm across comprise about 7% of the area. All have jagged margins bounded mainly by pyroxene "teeth", and some deviate

substantially from a circular shape (e.g. middle hole in Fig. 1a). Some plagioclase occurs as irregular, near-rectangular regions up to 2mm long containing pyroxene inclusions and having a jagged outline against bounding pyroxene grains (Fig. 1b). When the entire thin section is viewed at one time in a binocular microscope, those irregular regions give the impression of a ghostly variolitic texture. Under crossed polars at high magnification, the plagioclase lath-like regions are seen to consist of an intimate mosaic of small interlocking grains (Fig. 1c: see also [1] for an excellent illustration of the largest area of plagioclase). Other plagioclase grains occur interstitially to pyroxene grains as shown by the small white areas in Fig. 1a. Tridymite occurs as laths up to 2mm long peppered with small drops of plagioclase which based on electron microprobe scanning analyses comprise one-quarter of the volume (Fig. 2a). The laths are commonly associated with holes as in Fig. 1a. Some tridymite laths occur as pairs lying in a straight line on opposite sides of a hole (Fig. 1a), and the obvious interpretation is that the pairs are portions of a hexagonal plate penetrated by the hole. Other tridymite grains are tangential to cavities as though bubbles had stuck to tridymite plates during growth. Each tridymite lath actually consists of a mosaic of small interlocking grains with texture somewhat similar to that of the plagioclase mosaic.

The remaining 5% of the mode is composed of ilmenite—Ti-chromite intergrowths (Fig. 2d,e) sometimes showing subhedral boundaries suggesting sections through octahedral forms (Fig. 2c); a minor

occurrence is as small laths. Typically the opaque assemblage has pyroxene inclusions giving a "Swiss-cheese" texture. Trace phases include iron-troilite micrometer assemblages and iron associated with the opaque intergrowths. Several opaque intergrowths are rimmed by olivine. No additional phases were found in thin section, either optically or with the electron probe.

Careful examination of the small chips produced four additional mineral types or morphologies. Ilmenite, unlike that present in the thin-section, was found as thin, fragile tablets with mirror-like surfaces growing into two cavities; other similar grains were found among the single mineral grains. Ti-chromite showing stepped growth-faces was found in another cavity. Among the chips, three pale brown grains similar to pyroxene but without exsolution lamellae proved to be merrillite; although not observed in the cavities, the planar growth faces suggest uninhibited growth into cavities. Associated in a cavity with the Ti-chromite was a clear plagioclase grain with a euhedral form; one other similar occurrence was noted. All the above identifications were made from Gandolfi X-ray patterns and qualitative microprobe analysis.

Before going into details of the mineralogy it is obvious that the above textural features are very strange indeed, and cannot be explained by any single mechanism. Some coarse features (holes, indication of variolitic texture, platy and lathy overall shape of tridymite and plagioclase) are consistent with igneous crystallization, whereas some finer features, especially the chunky shape and coarse exsolution lamellae of the pyroxene grains, indicate a prolonged

metamorphic history. In addition, the mosaic extinction of the plagioclase and tridymite indicates yet a third process. The remainder of the description of the mineralogy is directed to obtaining information on the possible processes which transformed a presumed igneous texture into a more complex one.

3. Detailed Mineralogy

Quantitative energy dispersive (ED) analyses were obtained using a focused beam and on-line data reduction methods as described by Reed and Ware [4]. Minor elements were determined with crystal spectrometers using Albee-Ray correction factors. All analyses were referred to synthetic minerals of known compositions, and the analyses in Tables 1 and 2 have a detection level of 0.01 wt.% and an accuracy for major elements between 1 and 5% of the amount present. Single-crystal X-ray data were obtained from precession cameras.

Pyroxene. The exsolution lamellae are straight in most grains and range in width only two-fold. Very rare grains have curved lamellae as in Fig. 2a. Many grains are fractured.

Zero-layer precession photographs about the b-axis showed diffractions only from pigeonite ($P2_1/c$; a 9.69 b 8.97 c 5.22Å β 108.75°) and augite (C2/c; a 9.69 b 8.97 c 5.26 β 106.17°) with common (001).

X-ray scanning images showed clear lamellae with widths near
Table 1 5μm. Microprobe ED analyses (Table 1), obtained by maximizing or minimizing the Ca signal with a crystal spectrometer, cluster tightly

into high- and low-Ca groups at $En_{32}Fs_{27}Wo_{41}$ and $En_{40}Fs_{56}Wo_4$
Fig. 3 mol % (Fig. 3). The Ca content of the pigeonite may actually be even lower than 4% Wo because of systematic error from fluorescence and perhaps minor beam overlap. Minor elements show the usual trend for exsolved pyroxenes with Al,Ti and Cr strongly enriched in the augite and Mn in the pigeonite. Sodium and K in both pyroxenes were below 0.01 wt.%. The bulk composition, obtained by defocused beam analysis, $En_{37}Fs_{48}Wo_{15}$, corresponds to a Ca-rich pigeonite as the primary pyroxene before exsolution.

Plagioclase. Analyses for all textural varieties, including a grain from a vesicle, lie within the very narrow range An_{94-95}(mol %) with Mg 0.04 Fe 0.22 and K 0.04 wt.%. Two loose crystals were mounted on a precession camera; one showed very diffuse and elongated c and d diffractions (barely recognizable after 48 hr. exposure) and sharp a and b diffractions while the other showed sharp a,b,c and d diffractions similar to those of lunar plagioclase of near-equal composition [5].

Chromite and ilmenite. In each intergrowth, the chromite and ilmenite have constant compositions, but the compositions change from one
Table 2 Fig. 4 Fig. 5 intergrowth to another (Table 2, Figs. 4 and 5). Although there is no equilibrium over the entire thin section, local equilibrium is demonstrated by the constant partition of Mg between coexisting chromite and ilmenite. The MgO content of the ilmenite is low (<1.6%) consistent with the high bulk Fe/Mg of Ibitira. Although most Ti-chromites have high TiO_2 (~ 15-25%), one analysis (#4a, Table 2)

is unusually low (TiO_2 = 5.7%) and has high Cr_2O_3 (50.6); this grain is also unusual because it is not equidimensional, but lath shaped and included within tridymite. Fe-metal is common at grain boundaries within the ilmenite—Ti-chromite intergrowths. The one grain of Ti-chromite and those of ilmenite picked from cavities had compositions similar to the common matrix equivalents. Scanning X-ray images of a typical intergrowth are shown in Fig. 3d and e. Although some intergrowths show straight boundaries, most are curved. Spectrometer analyses of Zr showed strong partitioning into ilmenite. Values in the spinel phase ranged from <0.01 to 0.03 wt.% ZrO_2 and those in ilmenite from 0.08 and 0.18 wt.% ZrO_2, lower values being associated with spinel of lower TiO_2 content.

Fe-metal - This phase contains different Co and Ni depending on associated phases. Metal associated with troilite has Co ranging from 0.80 to 1.10 wt.% and Ni ~ 0.88 wt.%. Metal associated with ilmenite—Ti-chromite has slightly lower Co (0.40 - 0.60 wt.%) and much lower Ni (0.10 - 0.35 wt.%). Gandolfi patterns indicated kamacite.

Tridymite - Gandolfi X-ray patterns were like the Powder Diffraction File pattern 18-1170 for synthetic tridymite. Spectrometer data for minor elements were: FeO 0.33 Al_2O_3 0.27 CaO 0.20 K_2O 0.1 Na_2O 0.1 MgO < 0.01 wt.%.

Merrillite - Identification was made both by Gandolfi and precession photographs. Cell constants are a = 10.4 and c = 37.5Å. Compositional data, obtained only from unpolished grains gave: ED analysis; MgO 3.5 Al_2O_3 1.2 P_2O_5 44 CaO 44; spectrometer analysis SiO_2 0.5 FeO 1.89 La_2O_3 0.36 Ce_2O_3 0.80 Nd_2O_3 0.53 Sm_2O_3 0.19 Gd_2O_3 0.31 Dy_2O_3 0.08, other REE <0.05 wt.% each, F and Cl not detected, Σ 97.36. The low sum probably results from lack of polish. The term merrillite is used rather than whitlockite following the recommendations of Prewitt and Rothbard [6] as referred to the anhydrous nature of Ibitira and other eucrites.

Olivine - Narrow rims (~ 10μm) on some ilmenite—Ti-chromite intergrowths analyzed as Fe-rich olivine (Table 1, #8). The high TiO_2 and Cr_2O_3 may result from secondary fluorescence but because an analysis adjacent to ilmenite showed high Cr_2O_3 the olivine may really contain chromium.

4. Discussion

The above mineralogical features of the Ibitira eucrite, when examined in the context of data for other eucrites and howardites and for lunar samples, lead to a complex history. Perhaps the following sequence provides the simplest explanation:
(a) crystallization of the Ibitira eucrite in a lava flow producing a variolitic texture between pyroxene and plagioclase, chromite grains, and vesicles associated with plates of tridymite, (b) prolonged annealing which yielded a hornfelsic texture, coarse exsolution of the pyroxene (but not inversion of pigeonite to hypersthene) and ordering of the plagioclase; the coarse intergrowths of ilmenite and chromite with minor Fe-metal and Fe-rich olivine probably result from reduction of primary spinel during this period; vapor deposition

probably also occurred at this time, (c) strong shock sufficient to modify the texture of the plagioclase grains (perhaps involving local melting), but not sufficient to do more than bend or crack pyroxene grains, and (d) sufficient annealing to allow crystallization of the plagioclase as a sub-parallel mosaic and partial conversion to the low structural state. In the discussion, the evidence for this sequence will be examined in detail, especially in relation to the general features of eucrites, howardites and mesosiderites, ably summarized by Duke and Silver [7].

The simplest way to produce the rounded cavities i by presence of a gas phase, and the arguments of Wilkening and Anders [1] for CO are adopted. Shrinkage during metamorphism of a glassy, porous breccia might produce holes, but does not easily explain the associated plates of tridymite. Distortion of some of the holes and tridymite plates is easily explained by deformation. Perhaps the two plates in Fig. 1a were once one continuous plate, which was broken during deformation of the central cavity from an original spherical shape. If the holes are accepted as vesicles, restrictions are placed on the solidification regime of the parent magma. Although accurate modeling is impossible, one argument by Wilkening and Anders [1] for crystallization of the Ibitira eucrite in a thin flow some meters thick seems plausible: however, particle-track data should be inapplicable because of the prolonged metamorphism. By analogy with lunar mare basalts, a surface lava flow is most obvious, but a sub-surface dyke or sill cannot be ruled out because

the parent body may be small with a low gravitational gradient ($dP/dr = GMr^{-2}$ at the surface where P is gravitational pressure, r is radius, G gravitational constant, M mass).

The evidence for prolonged metamorphism is overwhelming, but it is difficult to quantify the conditions. No chemical zoning was found in the pyroxenes, and the compositions of the coexisting augite and pigeonite suggest equilibration halted near 950°C based on the data of Ishii et al. [8]. Evidence presented by Takeda et al. [9] indicated that Apollo 12 and 15 mare basalts cooled in lava flows up to 10m thick, but none of their pyroxenes show optically-visible exsolution in contrast to the relatively coarse exsolution of Ibitira pyroxenes. Unfortunately there is no evidence on the conditions under which metamorphism occurred. Perhaps the parent lava flow of the Ibitira eucrite was disrupted by impact, and the Ibitira eucrite was buried in a thick, hot ejecta blanket. This would be consistent with the general evidence from howardites and eucrites [7] for brecciation and recrystallization, and indeed fragments with hornfelsic or granoblastic texture set in a fine-grained matrix occur frequently in these meteorite groups. Another possibility might be intrusion as a dyke or sill well below the surface in a planetesimal, but not too deep to prevent vesiculation. If magma near 1200°C were injected into impact breccia at (say) 900°C, rapid crystallization would occur followed by annealing from ~ 1050°C downward.

Under equilibrium, tridymite should invert to high quartz upon cooling to 867°C [10], and preservation of tridymite might be taken to imply sufficiently rapid cooling below this temperature. Quartz

was reported in six eucrites, in two of which it occurred with tridymite and one with cristobalite, whereas tridymite was reported to occur alone in six others [summary in 7]. If this evidence were taken to indicate that transformation of tridymite to quartz is not kinetically inhibited, the presence of tridymite in the Ibitira eucrite would indicate rapid cooling through 867°C. The ferro-pigeonite in the Ibitira eucrite has not inverted to the orthorhombic variety, again suggesting absence of prolonged metamorphism at low temperature such as occurs in some regionally-metamorphosed rocks on Earth. Thus it might be suggested that the Ibitira eucrite cooled slowly down to ~ 950°C and then cooled more rapidly. However, there are many uncertainties behind this suggestion including lack of knowledge of kinetic factors and the possibility of inversion of tridymite to quartz in stage (b) followed by shock melting and recrystallization of tridymite in stages (c) and (d). Experimental data on kinetics of reactions in silica minerals and pyroxenes might allow quantification of the cooling conditions for the Ibitira eucrite. In the meantime, meaningful estimates of the physical conditions, such as the depth of burial in a possible ejecta blanket are impossible, though one might guess a depth nearer to 1km than 1m. The compositional and dimensional data of Ibitira pyroxenes are almost identical to rare pigeonite-augite pairs in 14310 [11,12] suggesting some similarity of thermal history. Furthermore the extent of exsolution in pyroxenes from all eucrites is roughly similar (Fig. 3; [8]).

The ilmenite—Ti-chromite-metal assemblage is similar to lunar examples where reduction or late stage re-equilibration has partially

transformed a Ti-rich spinel to a Ti-poorer spinel + ilmenite + metal [13]. Probably the reduction occurred during the metamorphism. Crystallization of minerals inside the vesicles probably occurred during the metamorphism because individual grains of chromite and ilmenite were found in the vesicles.

The third episode, that of shock, is inferred from the relative mineralogy of the pyroxene and plagioclase. During the prolonged metamorphism to about 950°C revealed by the pyroxene, the plagioclase should have transformed to a low structural state based on extrapolation of the kinetic data summarized by Smith [14]. The only feasible way to obtain the strange texture and the erratic structural disorder is by shock metamorphism followed by annealing. Pyroxene is much more resistant to shock than feldspar [15], as evinced by lunar fragments consisting of maskelynite and crystalline pyroxene. Fig. 2b illustrates an extreme example of shocked plagioclase (now maskelynite) in lunar sample 78482,5-A-15, illustrating the preservation of a metamorphic texture although highly shocked. Whether the Ibitira plagioclase was completely melted to maskelynite, or only partly converted from the crystalline to glassy state is undetermined, because a further episode of annealing occurred to provide crystallization or recrystallization of the plagioclase thereby obscuring the earlier state. This episode of annealing must be much less pronounced than the one invoked for the exsolution of the pyroxene. Because silica minerals and feldspars undergo shock melting at similar pressures, the present tridymite probably results from crystallization of shocked silica and is not the

original tridymite even though the original platy shape is fairly well preserved. The pyroxene underwent only fracturing and rare bending without any evidence of melting or reaction with the plagioclase. Shock melting of plagioclase and bending of pyroxene suggest that the Hugoniot pressure reached about 300kbar (3×10^{10}Pa).

How and when the shock metamorphism and subsequent annealing occurred is quite speculative. Of course, some event must be responsible for perturbation of the Ibitira meteorite into Earth-impacting orbit. However, once ejected into orbit the meteorite should cool rapidly to a very low temperature (< 100°K) by radiation loss, thereby precluding annealing in the temperature range for silicate reaction (over 800°K). This suggests that the Ibitira meteorite was shocked during an earlier event, and perhaps was annealed near the surface of a planetesimal prior to ejection into Earth orbit by a relatively mild event.

Whatever the actual details there can be no question that the Ibitira eucrite underwent a complex sequence of events, and that only a fortunate combination of such events allowed them to be disentangled from comparative mineralogy. Whether all these events occurred on one body, and whether all eucrites, howardites and mesosiderites derive from the same body is uncertain. We shall now compare the available mineralogical data to test the possibility of co-genesis, as suggested by Duke and Silver [7].

The Ibitira plagioclase is very calcic (An_{94}). This is at the calcic end of the main range An_{80-95} quoted by Duke and Silver, mainly from optical data, and is the same composition as the plagioclase

in the Moama eucrite for which detailed mineralogical data were given by Lovering [16]. The high Fe/Mg ratio in Ibitira anorthite (0.22/0.04) matches the high Fe/Mg ratio of the pyroxene (22/7) and contrasts with the more magnesian compositions of the Moama minerals (anorthite 0.09/0.08; pyroxene 19/11). The Fe and Mg contents of both anorthites are lower than for anorthite from lunar basalts; thus for plagioclase from Apollo 15 mare basalts [17], the Fe content is ~ 0.9 wt.% vs. 0.22 and 0.09 wt.%, respectively, for Ibitira and Moama anorthites. The obvious explanation for both eucrites is that metamorphic equilibration reduced the minor elements inferred to have been incorporated in the anorthites during original crystallization from a melt.

The Ibitira tridymite contains 25 wt.% inclusions of anorthite. This is much too high to be accounted for by exsolution, because Longhi and Hays [18] reported a maximum of 5 wt.% solution of anorthite molecule in silica minerals. Simultaneous crystallization of anorthite and tridymite followed by metamorphism provides a reasonable explanation [Longhi, pers. comm.]. Neither Duke and Silver nor Lovering reported inclusions of plagioclase in tridymite, but a systematic study would be worth-while in silica minerals from eucrites and howardites.

Fig. 4 summarizes the major elements in spinel-type phases from eucrites, and compares them with spinels from Apollo 15 basalts [19]. All the spinels from eucrites and mesosiderites lie close to a single trend from Ti-poor to Ti-rich compositions [20]. Lovering [16] reported that the chromite from Moama eucrite is very uniform, and

Bunch and Keil [20] reported only the mean composition for chromites in eucrites and mesosiderites, but mentioned up to 86% variation (mostly in Ti) of major elements from grain to grain in the eucrites and up to 13% in the mesosiderites. Bunch and Keil also reported composition variation within single grains, and coexistence with rutile and rarely ilmenite. Reexamination of the specimens is desirable to check whether all the chemical and mineralogical variations can be ascribed to different degrees of reduction of primary single-phase spinels (which would move the composition away from ulvöspinel) or whether the compositional range is the result mainly of primary crystallization. In Ibitira, the spinel with the least Ti occurs as a bladed crystal associated with ilmenite and enclosed in tridymite, and it has the same composition as the uniform spinel in Moama: however, the pyroxenes and plagioclases are distinctly different for these two eucrites as shown earlier. Whatever the details, the spinels from all the eucrites and mesosiderites fall into a single trend with all the spinels from mesosiderites lying at the Ti-poor region of the trend. Compared to the trend for Apollo 15 basalts, the eucrite-mesosiderite trend is poorer in Al and richer in Cr.

For Ibitira spinels, the distribution of Mg between coexisting ilmenite and spinel is monotonic and linear within experimental error. Analyses obtained by Bunch and Keil [20] for eucrites tend to lie around the trend for Ibitira, and the scatter may result from averaging for grains which do not touch each other. Only one point for the four mesosiderites lies near the trend. No ilmenite was

reported in the Moama eucrite, suggesting that the spinel phase had not been reduced.

The Ibitira pyroxenes fall neatly in the trend for pyroxenes from eucrites collected by Takeda et al. [21], and the Moama eucrite [16], and the trend of bulk compositions tends to lie parallel to but with lower Ca than the trend for Apollo 15 pyroxene-phyric basalts [22].

Merrillite has apparently not been reported from eucrites but the occurrence in Ibitira is compositionally similar to that of whitlockite in lunar rock 14310 [23]. The vesicular texture of Ibitira and the planar growth faces on merrillite strongly suggest vapor deposits similar to those found in lunar rocks [e.g. 24]. Other indications of vapor deposits are the euhedral crystals of ilmenite, ulvöspinel and plagioclase found in vugs. These were not seen in thin-section probably because they are too fragile. Compositionally these phases do not differ from those in the bulk rock which suggests equilibration between the vapor and the bulk rock.

A remarkable feature of the Ibitira eucrite is the absence of a late-stage KREEPy residuum such as is typically found in lunar basalts. Whether this feature is common to all eucrites and howardites is not clear from the literature, but should be checked carefully. It is consistent with the low content of large-ion-lithophile elements reported in bulk analyses of eucrites, and is one argument in favor of derivation of eucrites from an environment other than the Moon. The compositions of the metal and sulphide in the Ibitira and Moama eucrites fall in the range of those in

lunar basalts, and are consistent with presence of a late-stage, S-bearing, reducing vapor in all specimens.

There is a general tendency in the literature to explain the eucrite, howardite, diogenite and mesosiderite meteorites in terms of processes occurring in only one parent body. This is certainly the simplest assumption, but may be unwarranted. Furthermore there is a tendency to attempt interpretation of the mineralogy and petrology in terms of one trend of crystal-liquid differentiation (e.g. [25,26], and the chemistry in terms of one sequence of separation processes (e.g. [27]). These approaches are undoubtedly stimulating, but require some critical examination in the context of detailed mineralogical, petrological and chemical studies of all the above groups of meteorites on the level of examination of lunar samples. To raise just one question: why is there no significant Eu anomaly for the Ibitira and Juvinas eucrites [1] when the Fe-rich nature of their pyroxenes would indicate that they originated late in a crystal-liquid fractionation series after substantial amounts of plagioclase should have crystallized? There is no sense in an exhaustive discussion here of all the possible alternatives, and we conclude by re-emphasizing the problems with respect to interpretation of the petrogenesis, chemistry and particle tracks when there is so much evidence for complex, prolonged metamorphism associated with volatile movement and reduction.

Acknowledgements

We thank E. Anders and L. Wilkening for generously supplying the specimens and for discussion of the new results. We thank V. Baltuska, O. Draughn and T. Solberg for technical help. Financial aid is gratefully acknowledged from NASA 14-001-171 Res and NSF DMR72-03028 A04 (Materials Research Laboratory).

References

1 L. L. Wilkening and E. Anders, Some studies of an unusual eucrite: Ibitira, Geochim. Cosmochim. Acta 39 (1975) 1205-1210

2 T. E. Bunch, Petrography and petrology of basaltic achondrite polymict breccias (howardites), Proc. Lunar Sci. Conf. 6th, Geochim. Cosmochim. Acta 1, Suppl. 6 (1975) 469-492.

3 W. G. Melson and B. Mason, Lunar "basalts": some comparisons with terrestrial and meteoritic analogs, and a proposed classification and nomenclature, Proc. Second Lunar Sci. Conf., Geochim. Cosmochim. Acta 1, Suppl. 2 (1971) 459-467.

4 S. J. B. Reed and N. Ware, Quantitative electron microprobe analysis using a lithium drifted silicon detector, X-ray Spectrometry 2 (1973) 69-74.

5 I. M. Steele and J. V. Smith, Compositional and X-ray data for Luna 20 feldspar, Geochim. Cosmochim. Acta 37 (1973) 1075-1077.

6 C. T. Prewitt and D. R. Rothbard, Crystal structures of meteoritic and lunar whitlockites, Abstracts Sixth Lunar Sci. Conf. Houston (1975) 646-648.

7 M. B. Duke and L. T. Silver, Petrology of eucrites, howardites and mesosiderites, Geochim. Cosmochim. Acta 31 (1967) 1637-1665.

8 T. Ishii, M. Miyamoto and H. Takeda, Pyroxene geothermometry and crystallization-, subsolidus equilibration temperatures of lunar and achondritic pyroxenes, Abstracts Seventh Lunar Sci. Conf. Houston (1976) 408-410.

9 H. Takeda, M. Miyamoto, T. Ishii and G. E. Lofgren, Relative cooling rates of mare basalts at the Apollo 12 and 15 sites as estimated from pyroxene exsolution data, Proc. Lunar Sci. Conf. 6th Geochim. Cosmochim. Acta 1, Suppl. 6 (1975) 987-996.

10 O. F. Tuttle and N. L. Bowen, Origin of granite in the light of experimental studies in the system $NaAlSi_3O_8$-$KAlSi_3O_8$-SiO_2-H_2O, Geol. Soc. Amer., Mem. 74, (1958).

11 H. Takeda, M. Miyamoto and A. M. Reid, Crystal chemical control of element partitioning for coexisting chromite-ulvöspinel and pigeonite-augite in lunar rocks, Proc. Lunar Sci. Conf. 5th, Geochim. Cosmochim. Acta 1, Suppl. 5 (1974) 727-741.

12 H. Takeda and W. I. Ridley, Crystallography and chemical trends of orthopyroxene-pigeonite from rock 14310 and coarse fine 12033, Proc. Lunar Sci. Conf. 3rd, Geochim. Cosmochim. Acta 1, Suppl. 3 (1972) 423-430.

13 S. E. Haggerty, Apollo 14: subsolidus reduction and compositional variation of spinels, Proc. Lunar Sci. Conf. 3rd, Geochim. Cosmochim. Acta 1, Suppl. 3 (1972) 305-332.

14 J. V. Smith, Feldspar Minerals, Vol. 1, Springer (1974) 145-146.

15 D. Stöffler, Deformation and transformation of rock-forming minerals by natural and experimental shock processes. I. Behavior of minerals under shock compression, Fortschr. Miner. 49 (1972) 50-113.

16 J. F. Lovering, The Moama eucrite - a pyroxene-plagioclase adcumulate, Meteoritics 10 (1975) 101-114.

17 E. Dowty, M. Prinz and K. Keil, Composition, mineralogy and petrology of 28 mare basalts from Apollo 15 rake samples, Proc. Lunar Sci. Conf. 4th, Geochim. Cosmochim. Acta 1, Suppl. 4 (1973) 423-444.

18 J. Longhi and J. F. Hays, Solid solution and phase equilibria on the join anorthite-silica, Trans. Am. Geophy. Union 57 (1976) 304.

19 C. E. Nehru, M. Prinz, E. Dowty and K. Keil, Electron microprobe analyses of spinel group minerals and ilmenite in Apollo 15 rake samples of igneous origin, Univ. of N. Mexico Inst. Meteoritics Spec. Pub. 10 (1973).

20 T. E. Bunch and K. Keil, Chromite and ilmenite in non-chondritic meteorites, Am. Mineral. 56 (1971) 146-157.

21 H. Takeda, T. Ishii and M. Miyamoto, Characterization of crust formation on a parent body of achondrites and the Moon by pyroxene crystallography and chemistry, Abstracts Seventh Lunar Sci. Conf. Houston (1976) 846-848.

22 E. Dowty, K. Keil and M. Prinz, Lunar pyroxene-phyric basalts: crystallization under supercooled conditions, J. Petrol. 15 (1974) 419-453.

23 W. L. Griffin, R. Ämli and K. S. Heier, Whitlockite and apatite from lunar rock 14310 and from Ödegården, Norway, Earth Planet. Sci. Letters 15 (1972) 53-58.

24 D. S. McKay, U. S. Clanton, D. A. Morrison and G. H. Ladle, Vapor phase crystallization in Apollo 14 breccia, Proc. Lunar Sci. Conf. 3rd, Geochim. Cosmochim. Acta 1, Suppl. 3 (1972) 739-752.

25 T. S. McCarthy, A. J. Erlank and J. P. Willis, On the origin of eucrites and diogenites, Earth Planet. Sci. Letters 18 (1973) 433-442.

26 E. Stolper, Petrogenesis of eucrite, howardite and diogenite meteorites, Nature 258 (1975) 220-222.

27 J. Vizgirda and E. Anders, Composition of the eucrite parent body, Lunar Science VII, 898-900. Lunar Science Institute (1976).

TABLE 1. Ibitira pyroxene and olivine analyses

	Low-Ca Pyroxene			High-Ca Pyroxene			Ave. Pyx	Olivine
	(1)	(2)	(3)	(4)	(5)	(6)	(7)	(8)
MgO	13.0	13.0	13.1	10.3	10.6	10.9	12.2	6.76
Al_2O_3	0.23	0.23	0.25	1.28	1.50	1.60	0.55	nd
SiO_2	50.7	50.4	50.1	50.1	50.1	50.6	50.3	32.1
CaO	1.71	2.03	2.39	18.9	19.7	19.9	7.12	0.13
TiO_2	0.46	0.46	0.50	1.02	1.02	0.97	0.66	0.42*
Cr_2O_3	nd	nd	nd	0.51	0.29	0.42	0.39	1.04*
MnO	0.84	0.96	0.77	nd	0.29	0.37	0.77	0.84
FeO	34.0	33.6	31.9	16.4	16.1	16.2	28.4	60.2
Σ	100.94	100.68	99.01	98.51	99.60	100.96	100.39	101.49
	cations based on 6(Ox)							
Mg	0.761	0.765	0.775	0.598	0.612	0.622	0.711	0.633
Al	0.011	0.011	0.012	0.059	0.68	0.071	0.025	-
Si	1.990	1.980	1.994	1.954	1.934	1.928	1.970	2.017
Ca	0.071	0.085	0.102	0.789	0.816	0.814	0.299	0.008
Ti	0.014	0.013	0.015	0.030	0.030	0.028	0.019	0.020
Cr	-	-	-	0.016	0.008	0.013	0.012	0.052
Mn	0.028	0.032	0.026	-	0.009	0.012	0.025	0.044
Fe	1.116	1.104	1.061	0.535	0.520	0.515	0.930	3.163
En	39.0	39.1	40.0	31.1	31.4	31.9	36.7	Fo 16.7
Fs	57.3	56.5	54.7	27.8	26.7	26.4	47.9	Fa 83.3
Wo	3.7	4.4	5.3	41.1	41.9	41.7	15.4	

*Values high due to secondary fluorescence of Cr-ulvöspinel.
nd not detected.

TABLE 2. Ibitira Ti-chromite and ilmenite analyses.

Ti-chromite

	(1a)*	(2a)	(3a)	(4a)	(5a)	(6a)	(7)	(8)	(9)
MgO	0.82	0.78	0.45	1.31	0.59	0.98	0.58	1.39	2.38
Al_2O_3	4.79	3.30	4.18	7.60	4.44	5.49	4.32	3.01	7.72
TiO_2	17.6	24.5	19.8	5.71	18.8	14.7	19.0	23.8	5.39
Cr_2O_3	30.5	20.4	26.4	50.6	28.3	36.9	28.7	19.8	50.10
MnO	nd	nd	0.65	nd	0.01	0.53	0.38	0.71	0.81
FeO	47.3	52.9	49.0	34.7	48.4	43.5	48.8	50.6	32.67
Σ	101.01	101.88	100.48	99.92	101.14	102.1	101.78	99.31	99.74
	Atoms based on 12(Ox)								
Mg	0.130	0.123	0.071	0.207	0.093	0.154	0.092	0.226	0.375
Al	0.605	0.414	0.535	0.951	0.563	0.682	0.544	0.388	0.961
Ti	1.419	1.958	1.614	0.456	1.522	1.166	1.527	1.959	0.428
Cr	2.587	1.720	2.260	4.246	2.406	3.076	2.425	1.717	4.186
Mn	-	0.052	0.059	-	0.056	0.047	0.034	0.065	0.072
Fe	4.243	4.708	4.448	3.084	4.352	3.830	4.365	4.632	2.887

Ilmenite

	(1b)*	(2b)	(3b)	(4b)	(5b)	(6b)	(7)	(8)
MgO	1.00	1.09	0.58	1.54	0.91	1.18	1.58	1.42
TiO_2	54.2	54.6	53.8	53.7	54.5	54.0	53.2	52.2
MnO	0.51	0.47	0.47	0.64	0.53	0.61	0.36	0.59
FeO	45.4	44.5	45.1	43.3	45.4	43.4	43.1	42.9
Σ	101.11	100.66	99.95	99.18	101.34	99.19	98.24	97.11
	Atoms based on 12(Ox)							
Mg	0.147	0.159	0.087	0.230	0.133	0.176	0.238	0.217
Ti	4.028	4.020	4.049	4.045	4.033	4.068	4.031	4.028
Mn	0.043	0.039	0.040	0.054	0.044	0.051	0.030	0.051
Fe	3.755	3.641	3.775	3.626	3.736	3.636	3.629	3.676
Σ R^{+2}	3.945	3.839	3.902	3.910	3.913	3.863	3.897	3.944

*a and b denote coexistence in same intergrowths. Analyses 7 and 8 are from separate grains. Analyses 9 is average chromite in Moama [16]; total includes 0.67 V_2O_3.

FIGURE CAPTIONS

Fig. 1 Textures in Ibitira eucrite.

(a) This 4 x 1.5mm montage taken in plain light shows three cavities now filled with epoxy. The texture is dominated by pyroxene (grey) with fine exsolution lamellae just at the limit of optical resolution. White areas are plagioclase and the black area at lower left is chromite-ilmenite intergrowth with pyroxene inclusions. Particularly emphasized are four laths with irregular boundaries outlined in ink for clarity. These are interpreted as sections of two plates of tridymite with plagioclase inclusions; see text for suggestion that they once formed one plate.

(b) Plagioclase "lath" with pyroxene inclusions and irregular boundary with pyroxene grains. Black areas are chromite-ilmenite intergrowths. The speckled irregular lath pointing NW from the middle of the right-hand edge is tridymite with plagioclase inclusions. Plain light, 1.1mm wide.

(c) Central part of plagioclase "lath" at high magnification and under crossed polars. 0.15mm wide.

Fig. 2 Textures in Ibitira eucrite and lunar soil fragment.

(a) The speckled lath is tridymite containing drop-like inclusions of anorthite. Grey grains with lamellae are pyroxene: note curvature of some lamellae especially near the arrow. Clear grains are anorthite. Plain light, 0.4mm wide.

(b) Lunar soil fragment 78482,5-A-15 showing euhedral maskelynite (light grey with speckling from epoxy in thin section), pyroxene (dark grey) and opaque phases. Plain light, 0.5mm wide.

Fig. 2 (continued)

(c) Intergrowth of Ti-chromite and ilmenite (both light grey) showing subhedral outline against pyroxene (dark grey) and containing pyroxene inclusions. Reflected light, 0.5mm wide.

(d) and (e) Cr and Ti X-ray scanning images (K_α radiation) of intergrown Ti-chromite and ilmenite. Absence of both Cr and Ti identifies areas of sub-rounded pyroxene inclusions, while absence of just Cr identifies ilmenite. 0.25mm wide.

Fig. 3 Pyroxene compositions for representative eucrites. Bulk compositions are shown by solid symbols and exsolved phases by open symbols. Actual samples usually showed some variation and low-Ca compositions may be too high in Ca because of overlap and fluorescence. Samples labeled by (1) and (3) are from [21], and (2) from [16]. General crystallization trend of Apollo 15 pyroxene-phyric basalts [22] is shown for comparison.

Fig. 4 Mg in ilmenite vs. Mg in coexisting Ti-chromite calculated for 12 oxygens. Data for other eucrites and mesosiderites from [20].

Fig. 5 Spinel-phase compositions in Ibitira compared to those in other eucrites and mesosiderites, and from compositionally similar Apollo 15 basalts. Meteoritic and lunar data define similar near-linear trends with nearly constant Cr/Al. Note tendency for most meteoritic specimens to have low Ti. Data for Moama from [16], other meteorites from [20], and lunar trend from [19].

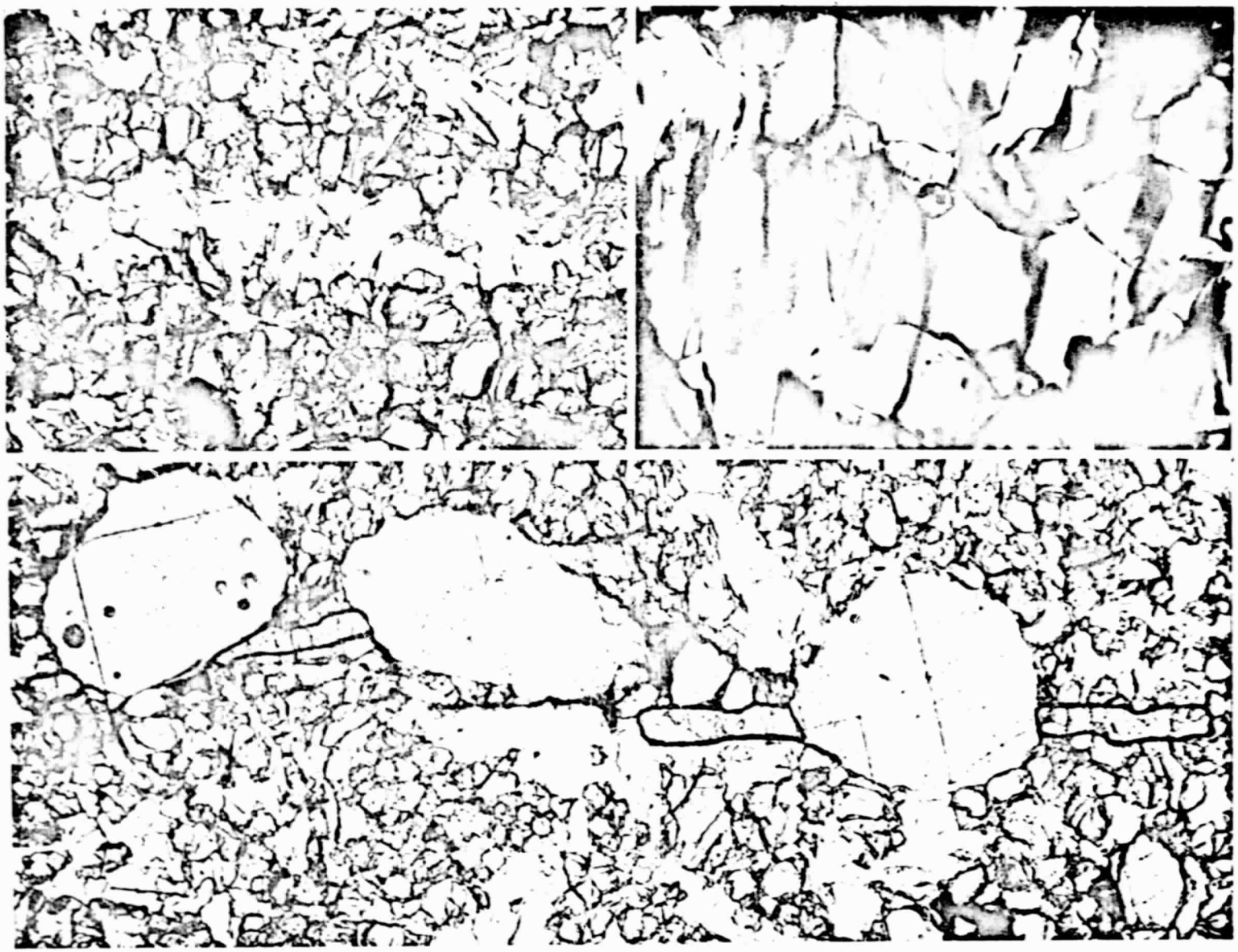

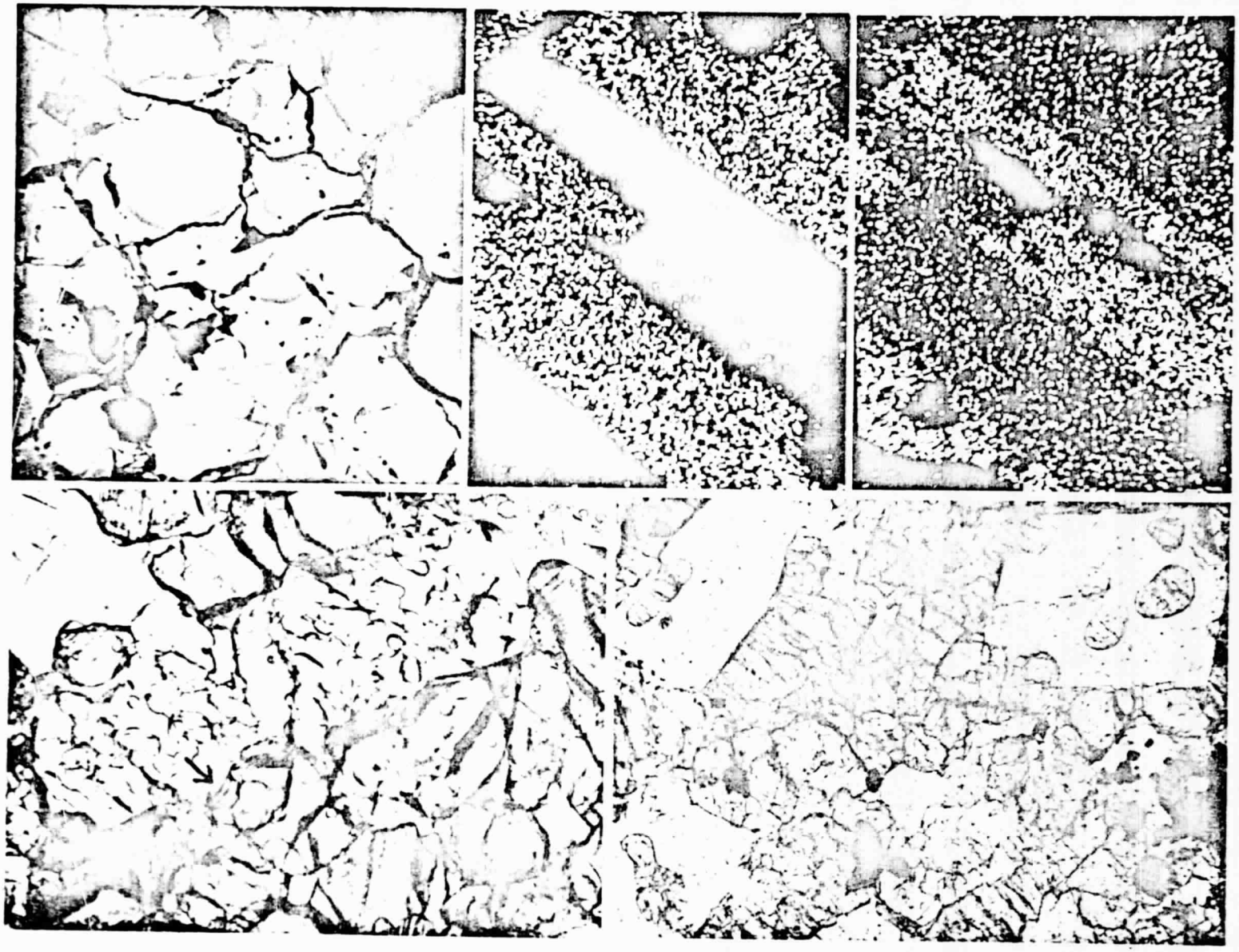

Fig 3 Steele et al. II

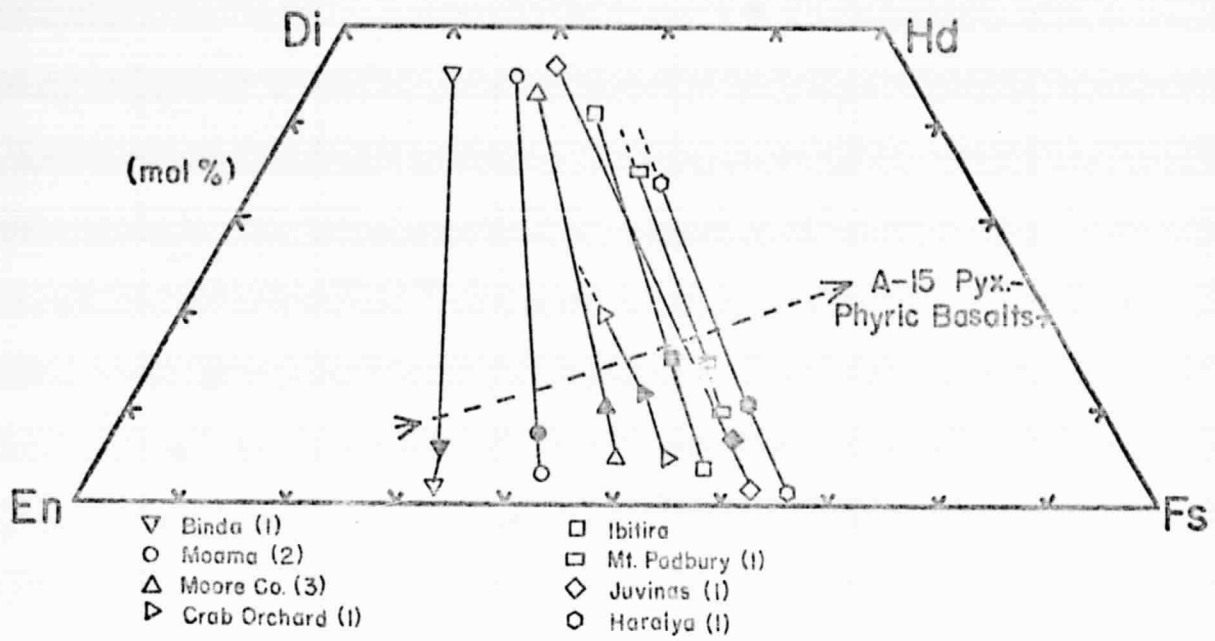

Fig 4 Steele and Smith

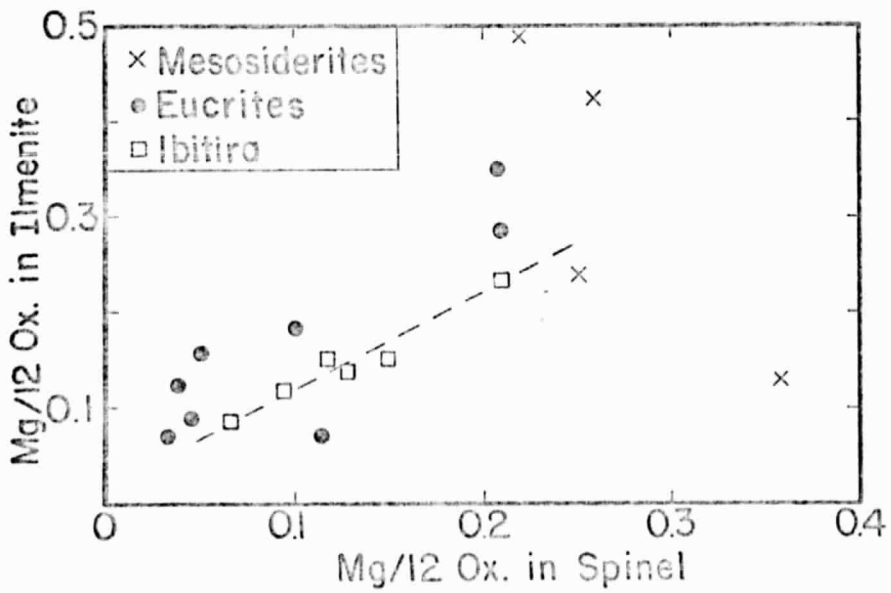

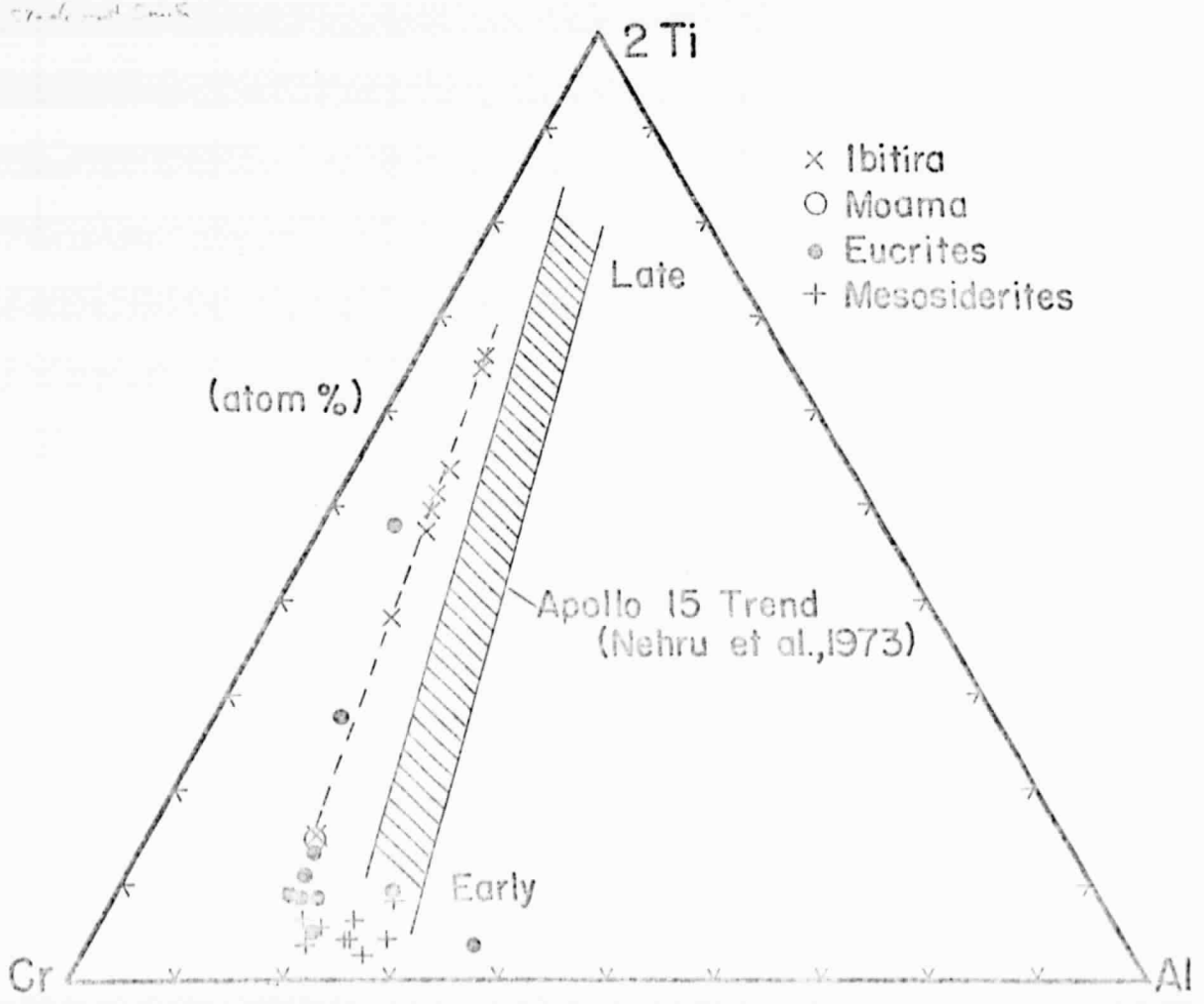
2 Ti
× Ibitira
O Moama
• Eucrites
+ Mesosiderites
Late
(atom %)
Apollo 15 Trend
(Nehru et al., 1973)
Early
Cr
Al